

Supporting Information

Helical Mesoscopic Crystals Based on Achiral Charge-Transfer Complex with Controllable Untwisting/Breaking

Canglei Yang, Lixing Luo, Jinqiu Chen, Bo Yang, Wei Wang, Hebin Wang, Guankui Long, Guangfeng Liu, Jing Zhang* and Wei Huang*

***Jing Zhang** - State Key Laboratory of Organic Electronics and Information Displays & Institute of Advanced Materials (IAM), Nanjing University of Posts & Telecommunications, 9 Wenyuan Road, Nanjing 210023, China;
E-mail: iamjingzhang@njupt.edu.cn.

***Wei Huang** - Frontiers Science Center for Flexible Electronics (FSCFE), MIT Key Laboratory of Flexible Electronics (KLoFE), Shaanxi Key Laboratory of Flexible Electronics, Xi'an Key Laboratory of Flexible Electronics, Xi'an Key Laboratory of Biomedical Materials & Engineering, Xi'an Institute of Flexible Electronics, Institute of Flexible Electronics (IFE), Northwestern Polytechnical University, Xi'an 710072, China;
E-mail: provost@nwpu.edu.cn.

Table of Contents

Experimental Procedures	3
Materials	3
Polymorphic Crystals Growth and Structural Analysis	3
Selective Growth of the Form 1 and 2 Micro/nanocrystals on the Substrates	3
Phase transition induction of helical crystal	3
Measurements	3
Theoretical Calculation Details	3
Results and Discussion	4
Fig S1. XRD patterns of pyrene, DTTCNQ and Form 1 cocrystal	4
Fig S2. Left-handed and right-handed helical conformations simultaneously existed in the crystal morphology	4
Fig S3. The number distribution of spiral crystals in different thickness ranges	5
Fig S4. Optical microscope pictures of pyrene-DTTCNQ crystals grown from toluene, chlorobenzene, chloroform, acetonitrile and DMF solutions by drop casting method. Polarity rankings of different solvents	5
Fig S5. Photo images of needle-shaped Form 1 and rod-shaped Form 2 cocrystals	6
Fig S6. Structural drawings of Form 1 and Form 2	6
Fig S7. The dihedral angle in DTTCNQ molecule of Form 1 and Form 2 between four cyano units and fused-ring quinone core plane	7
Fig S8. The calculated Mulliken charge distribution of Form 1 and Form 2 cocrystals at the DFT level with B3LYP/6-31G*	7
Fig S9. Thermal profile of pyrene-DTTCNQ cocrystal with rate of 5 °C/min during the heating procession	8
Fig S10. Changes of different molecular bonds and twist angles in the DTTCNQ molecules of Form 1 and Form 2	8
Table S1. Crystal data and structure refinements for Form 1 and 2 cocrystals	9
Table S2. The relative energy of the two cocrystals	10
Table S3. The crystal structure changes of Form1 and Form 2 before and after phase transformation, including cell parameters, bond length, bond Angle and other key parameters	10

Experimental Procedures

Materials. Pyrene and DTTCNQ purchased from Luminescence Technology Corp were used directly as received without further purification. All solvents were HPLC grade.

Polymorphic Crystals Growth and Structural Analysis. Using hot acetonitrile solution as raw material, Form 1 and Form 2 complexes were prepared by different methods. First, dissolve the mixture of pyrene and DTTCNQ (molar ratio of 1:1) in acetonitrile to obtain a solution with a concentration of 0.6 mg/mL. After heating at 70 °C for 1 hour to ensure complete dissolution, the mixed solution was allowed to stand on the table for about 3 hours, and the black needle-like compound Form 1 finally settled on the bottom of the bottle. If the solution is left to stand for a long time of more than a week, rod-shaped Form 2 cocrystals would be produced. In addition, Form 1 can be frozen at -20 °C for more than one week to obtain Form 2, but the purity is not as high as the former way. Subsequently, the needle-shaped and rod-shaped cocrystals were filtered from the solution and dried in the air. The Bruker smart-1000-CCD diffractometer with graphite-monochromatic Mo K α radiation ($\lambda = 0.71073$ Å) was used to measure the crystal structures of Form 1 and Form 2 single crystals. X-ray crystallography data was collected at room temperature. The X-ray crystallographic data were collected at room temperature. The structure was resolved by the direct method and refined by the full-matrix least-squares method on F^2 using the SHELXL-97 program.

Selective Growth of the Form 1 and 2 Micro/nanocrystals on the Substrates. In order to grow micro/nano crystals on the substrate, an acetonitrile/chloroform/acetonitrile/DMF solution (0.3 mg/mL) containing pyrene and DTTCNQ in a molar ratio of 1:1 was drop-cast onto the SiO₂/Si substrate. As the solvent evaporates, ribbon/wire-shaped Form 1 crystallites were prepared on the substrate. For Form 2 micro/nano crystals preparation, the substrate with Form 1 needs to be placed in an environment of -20 °C for more than a week or be repeatedly cooled (-20 °C) and heated (room temperature) seven to eight times.

Phase transition induction of helical crystal. Phase transition induction trace of twisted Form 1 micro/nano ribbon and nanowire was directly conducted on the aforementioned substrate with a microscope. For free-standing observation, a small amount of 0.3 mg/mL acetonitrile (10 μ L) solution was dropped onto the substrate and before full evaporation 50 μ L ethanol was dropped onto the surface for nanocrystal immersion and transfer, then the helical crystals in ethanol were observed with optical microscope. During the temperature control process, a temperature control table was used to lower the temperature to -20 °C and then increased it at a rate of 5 °C/min in order to clear phase transition induction.

Measurements. The nanostructures of the two phase complexes were characterized by optical microscopy (BX53, Olympus), UV-visible absorption spectrum (UV-vis spectra, LAMBDA 35), Atomic force microscopy (AFM, Bruker Dimension Icon), Scanning electron microscope (SEM, S4800), Transmission electronic microscopy (TEM, HITACHI HT7700) and corresponding selected-area electron diffraction (SAED, HITACHI HT7700). The DSC analysis were recorded on DSC2A-01130 at a temperature ramp of 10 °C/min under N₂. PXRD was measured on a D/max2500 with Cu K α source ($\kappa = 1.541$ Å).

Theoretical Calculation Details. The crystal structures of the co-crystals were optimized by using VASP 5.4 (Vienna Ab initio Simulation Package) program within the Perdew-Burke-Ernzerhof (PBE) functional.¹⁻³ The reciprocal space was covered by a Γ -centered Monkhorst-Pack lattice of $3 \times 3 \times 3$ K-points. The convergence criteria were set to 10^{-5} eV for the SCF and -0.001 eV Å⁻¹ for the geometry optimization.

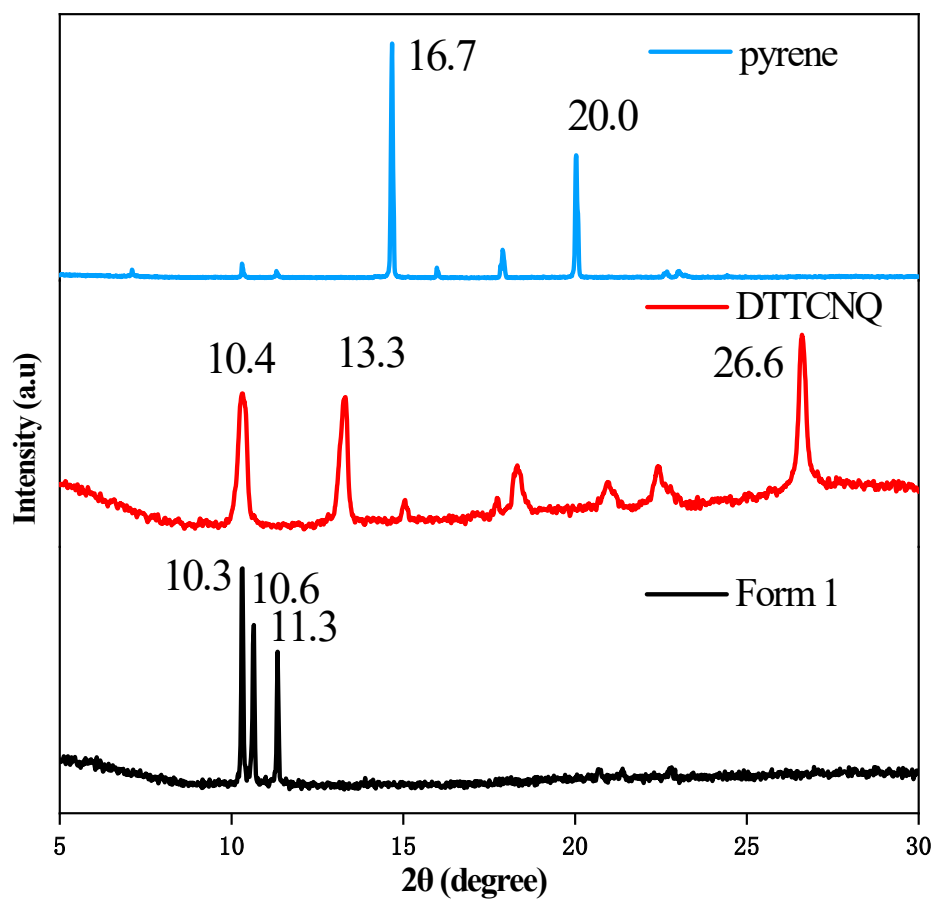


Fig S1. XRD patterns of pyrene, DTTCNQ and Form 1 cocrystal.

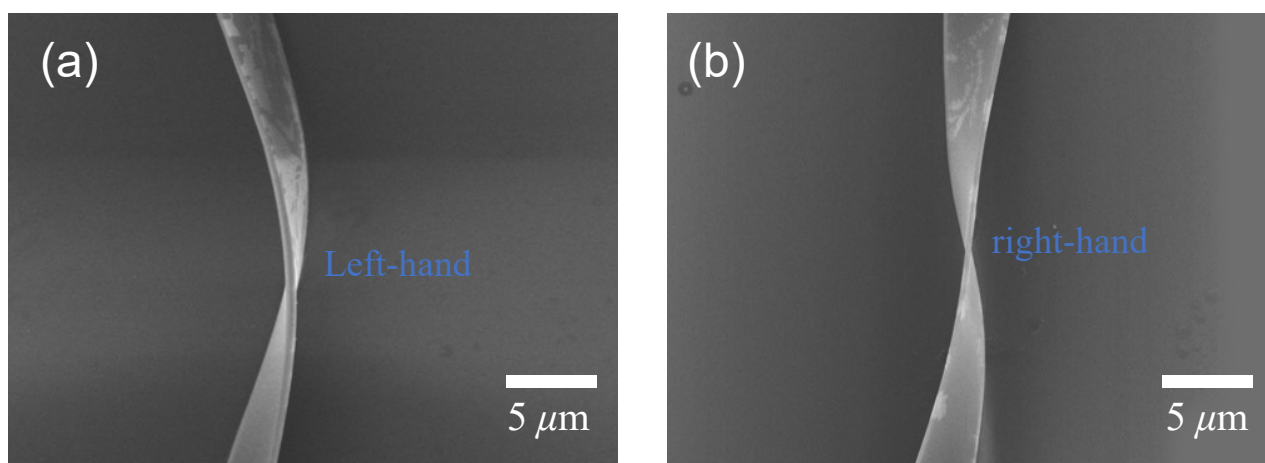


Fig S2. (a) Left-handed and (b) right-handed helical conformations simultaneously existed in the crystal morphology.

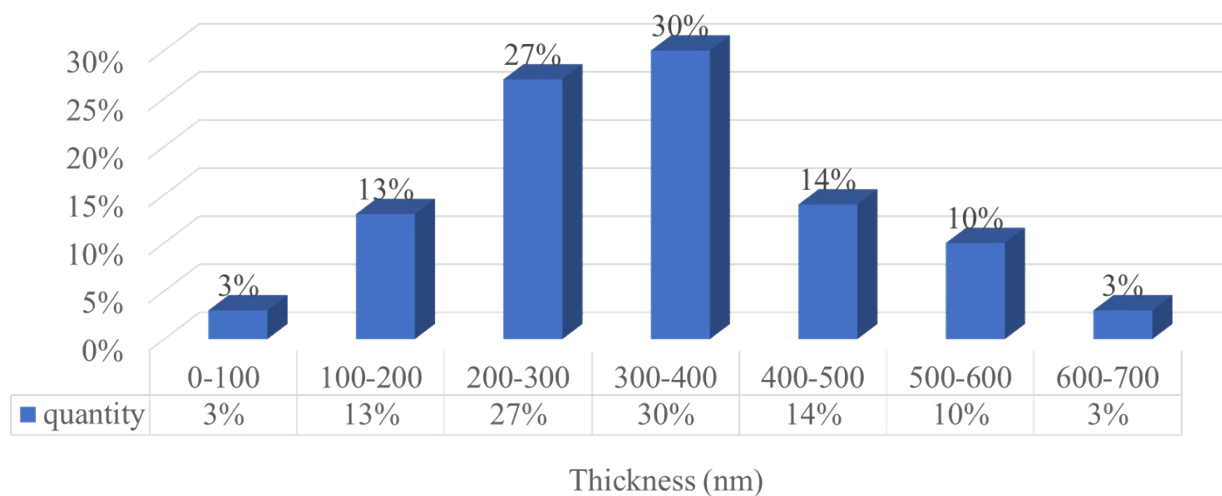


Fig S3. The number distribution of spiral crystals in different thickness ranges.

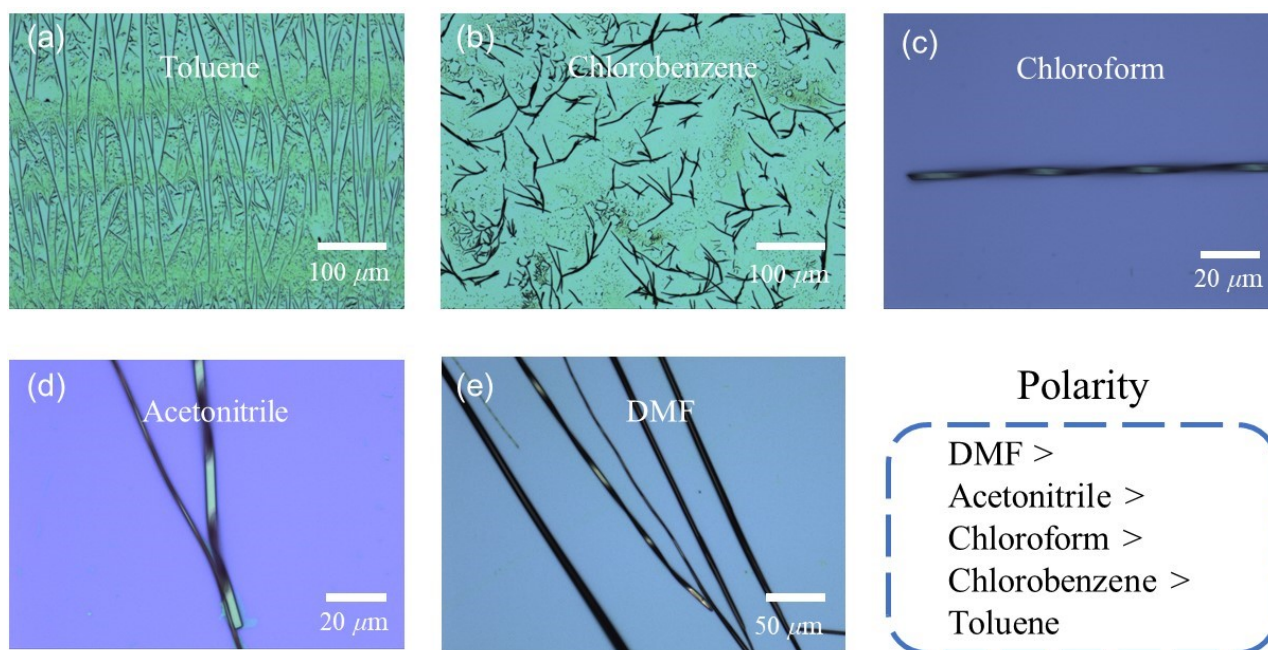


Fig S4. Optical microscope pictures of pyrene-DTTCNQ crystals grown from (a) toluene, (b) chlorobenzene, (c) chloroform, (d) acetonitrile and (e) DMF solutions by drop casting method.

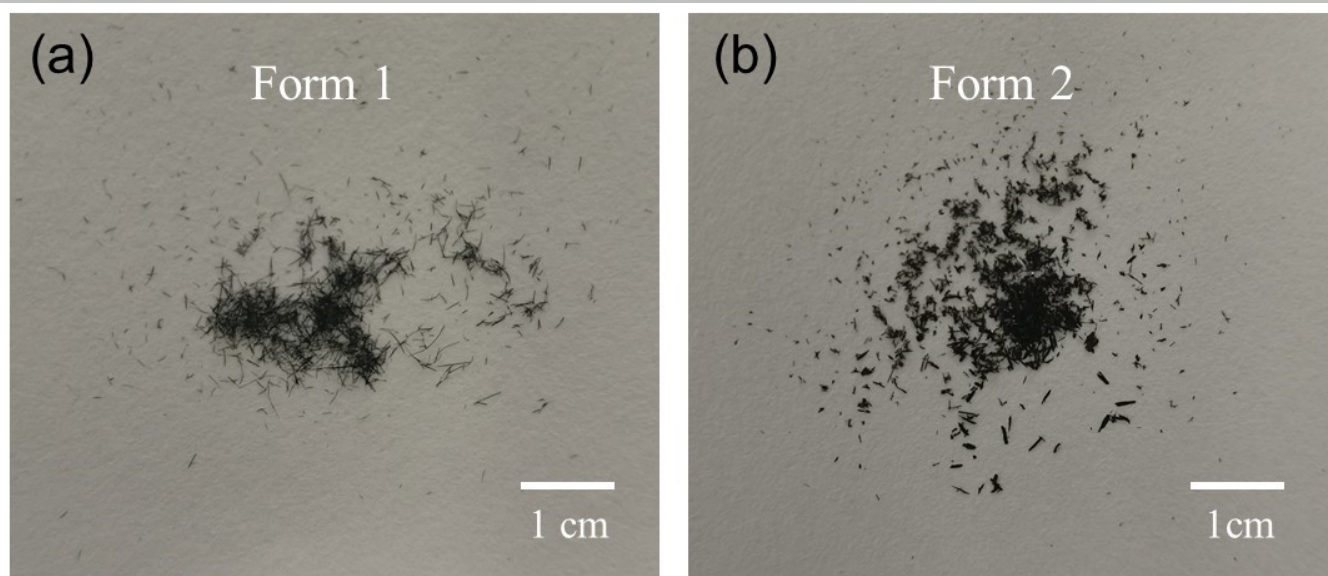


Fig S5. Photo images of (a) needle-shaped Form 1 and (b) rod-shaped Form 2 cocrystals.

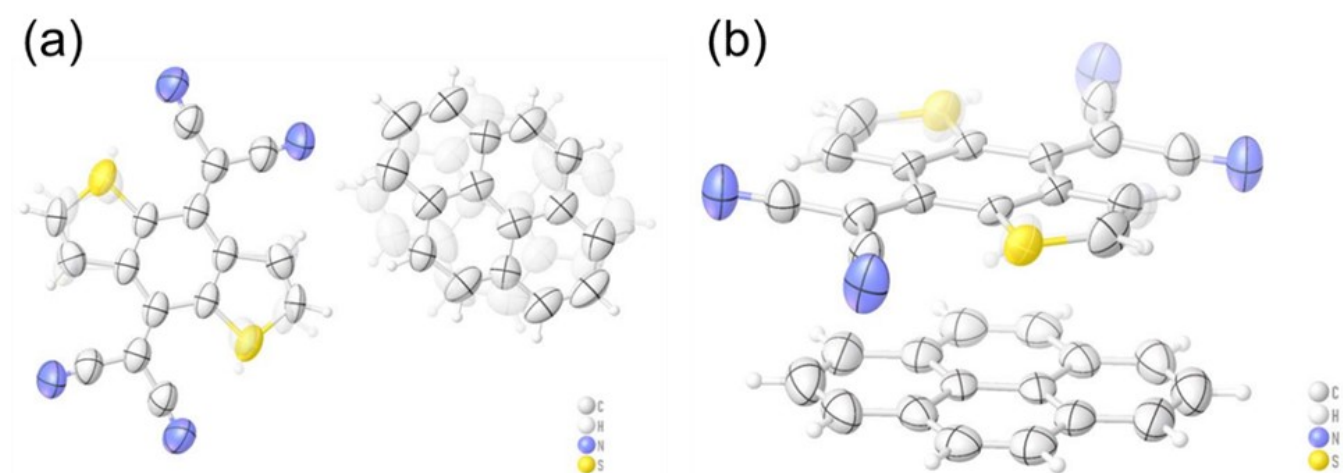


Fig S6. Structural drawings of (a) Form 1 and (b) Form 2.

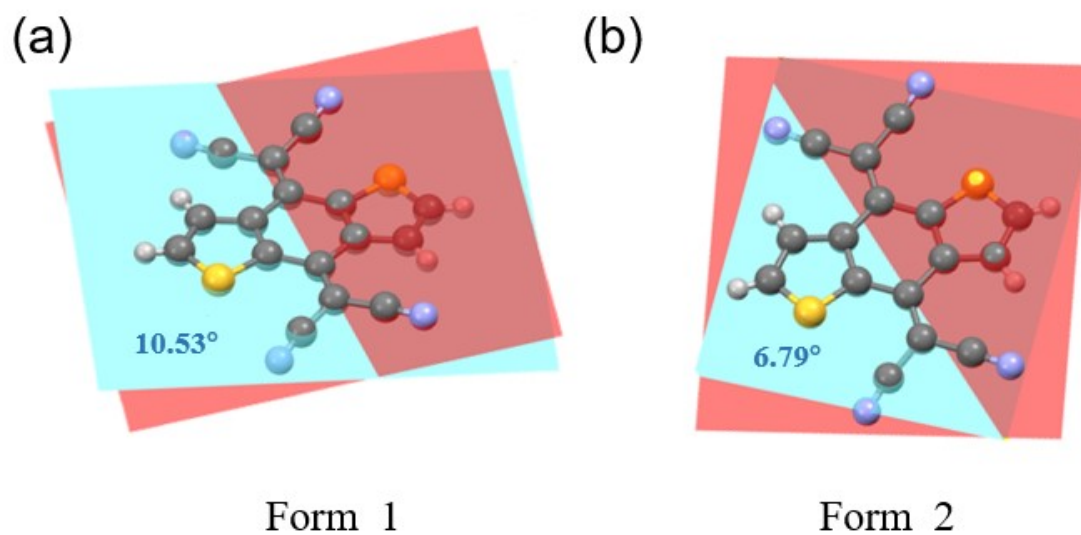


Fig S7. The dihedral angle in DTTCNQ molecule of (a) Form 1 and (b) Form 2 between four cyano units and fused-ring quinone core plane.

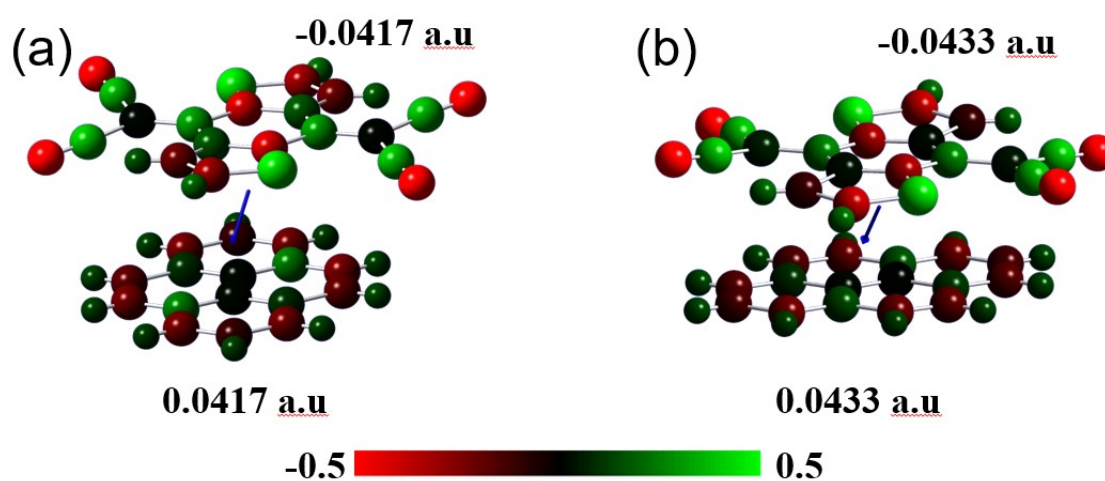


Fig S8. The calculated Mulliken charge distribution of (a) Form 1 and (b) Form 2 cocrystals at the DFT level with B3LYP/6-31G*.

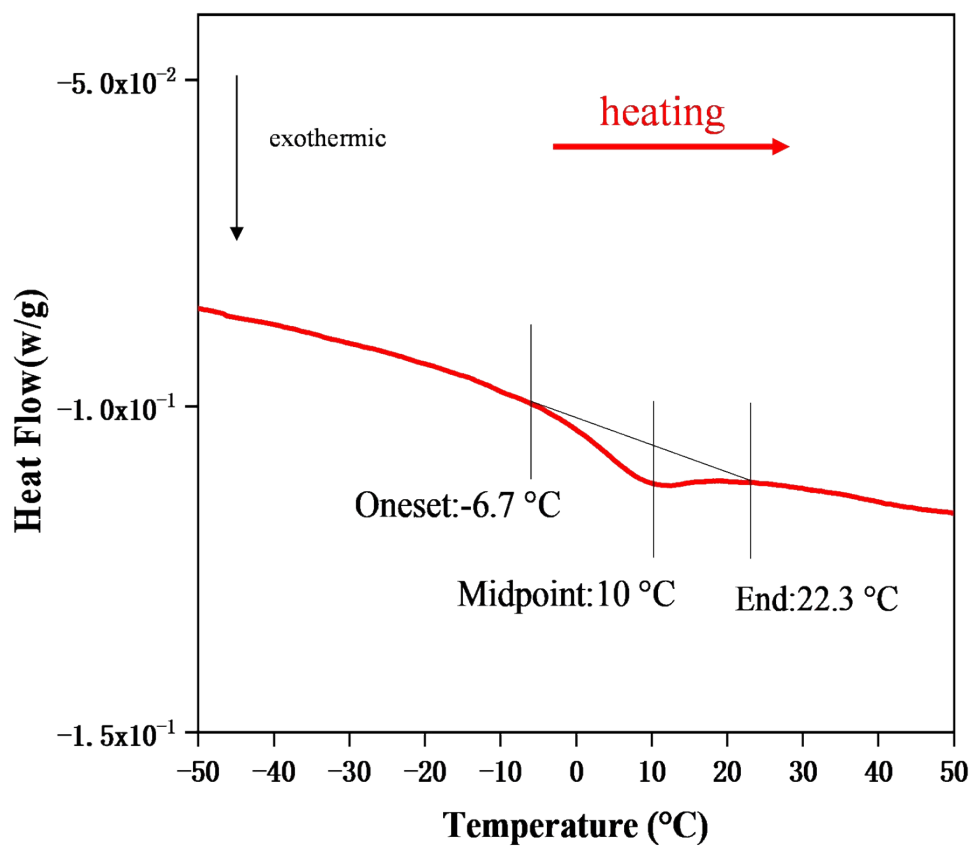


Fig S9. Thermal profile of pyrene-DTTCNQ cocrystal with rate of 5 °C/min during the heating procession.

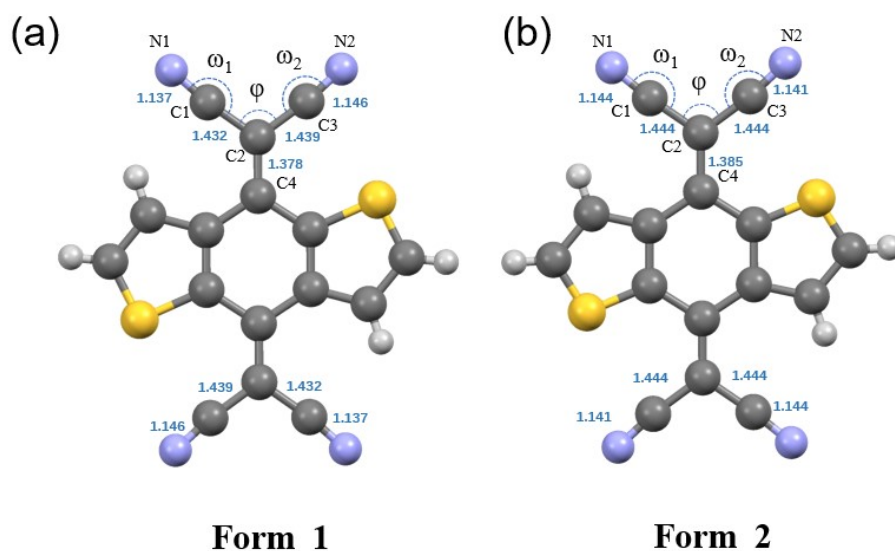


Fig S10. Changes of different molecular bonds and twist angles in the DTTCNQ molecules of Form 1 (a) and Form 2 (b).

Table S1. Crystal data and structure refinements for Form 1 and 2 cocrystals.

	Form 1	Form 2
Formula	$C_{32}H_{14}N_4S_2$	$C_{32}H_{14}N_4S_2$
Formula weight	518.59	518.62
Temperature (K)	292	292
Wavelength (Å)	0.71073	0.71073
Crystal system	triclinic	triclinic
space group	<i>P</i> -1	<i>P</i> -1
Unit cell dimensions		
<i>a</i> (Å)	7.492(4)	7.551(5)
<i>b</i> (Å)	9.468(5)	9.095(6)
<i>c</i> (Å)	9.682(5)	9.799(7)
α (°)	112.930(2)	67.642(13)
β (°)	109.052(2)	86.816(15)
γ (°)	90.147(2)	74.351(14)
Volume (Å ³)	591.24(5)	598.5(7)
<i>Z</i>	1	1
Absorption coefficient (mm ⁻¹)	2.286	0.253
<i>F</i> (000)	266.0	266.0
Crystal size (mm)	0.200 x 0.130 x 1.20	0.190 x 0.180 x 0.170
θ range (°)	5.12 to 68.64	2.25 to 25.00
Limiting indices	$-9 \leq h \leq 9$ $-11 \leq k \leq 11$ $-11 \leq l \leq 11$	$-8 \leq h \leq 8$ $-10 \leq k \leq 10$ $-11 \leq l \leq 8$
Reflections collected	12390	1172
<i>R</i> (int)	0.0538	0.0670
Absorption correction		Semi-empirical from equivalents
Refinement method		Full-matrix least-squares on F^2
Data / restraints / parameters	2181 / 195 / 247	2034 / 129 / 191
<i>R</i> [<i>I</i> > 2sigma(<i>I</i>)]	$R_1 = 0.0606$ $wR_2 = 0.1963$	$R_1 = 0.0823$ $wR_2 = 0.2149$
<i>R</i> (all data)	$R_1 = 0.0679$ $wR_2 = 0.2071$	$R_1 = 0.1339$ $wR_2 = 0.2339$
Goodness-of-fit on F^2	1.172	0.999
CCDC NO.	2089461	2089463

Table S2. The relative energy of the two cocrystals.

	Energy (eV)	Relative energy (meV/atom)
Form 1-a	-376.931	0
Form 1-b	-376.956	-0.487
Form 2-a	-376.981	-0.961
Form 2-b	-376.977	-0.887

Table S3. The crystal structure changes of Form1 and Form 2 before and after phase transformation, including cell parameters, bond length, bond angle and other key parameters.

	Form 1	Form 2	Δ ^[a]
<i>a</i> (Å)	7.492	7.511	0.019
<i>b</i> (Å)	9.468	9.799 ^[b]	0.331
<i>c</i> (Å)	9.682	9.096 ^[c]	-0.587
<i>d</i> _{A-D-A} (Å)	7.030	6.975	-0.055
<i>d</i> _{D-A-D} (Å)	6.983	6.874	-0.109
θ (°) ^[d]	10.53	6.79	-3.74
<i>d</i> ₁ (Å) ^[e]	1.137 & 1.146	1.144 & 1.141	0.007 & -0.005
<i>d</i> ₂ (Å) ^[f]	1.432 & 1.439	1.444 & 1.444	0.012 & 0.005
<i>d</i> ₃ (Å) ^[g]	1.378	1.385	0.007
ω_1 & ω_2 (°) ^[h]	174.14 & 173.60	173.06 & 175.36	-1.08 & 1.76
φ (°) ^[i]	109.29	109.52	0.23

[a] Δ represents the difference between the first two values. Since the *b* and *c* axes of Form 1 correspond to the *c* and *b* axes of Form 2, [b] and [c] are the *c*-axis and *b*-axis edge lengths of the unit cell of Form 2 respectively. [d] θ represents the dihedral angle between the plane of the four cyano groups and the fused ring quinone. [e-g] *d*₁, *d*₂ and *d*₃ represent the covalent bond length of C1≡N1 & C3≡N2, C1-C2 & C2-C3, C2-C4, respectively. [h] ω_1 and ω_2 denotes the torsion angle between C1≡N1 and C1-C2, C3≡N2 and C2-C3. [i] φ denotes the torsion angle between C1-C2 and C2-C3. Atomic number and some parameters can refer to Supporting Information.

References

- (1) P. E. Blöchl, *Phys. Rev. B*, 1994, **50**, 17953-17979.
- (2) G. Kresse, and J. Hafner, *J. Phys.; Condens. Matter*, 1994, **6**, 8245.
- (3) G. Kresse, and J. Furthmüller, *Comp. Mater. Sci.*, 1996, **6**, 11-50.